


Research Article

Acoustic Radiation Performance of a Composite Laminated Plate Subjected to Local Temperature

Yonggan Sun ^{1,2} and Yong Xiao^{1,2}

¹School of Civil Engineering, Chongqing Jiaotong University, Chongqing 400074, China

²Chongqing Steel Structure Industry Limited Company, Chongqing 400000, China

Correspondence should be addressed to Yonggan Sun; sunygqj@163.com

Received 15 August 2021; Revised 23 April 2022; Accepted 27 April 2022; Published 1 August 2022

Academic Editor: Valeria Vignali

Copyright © 2022 Yonggan Sun and Yong Xiao. This is an open access article distributed under the Creative Commons Attribution License, which permits unrestricted use, distribution, and reproduction in any medium, provided the original work is properly cited.

Composite structures are extensively applied because of their high specific stiffness-to-weight ratios and other advantages. In various scenarios, composite structures are elastically coupled and usually exposed to a nonuniform thermal environment. This paper presents numerical simulation studies on the vibroacoustic characteristics of a composite laminated plate with elastic supports subjected to local temperature. The thermal stiffness matrix and stiffness matrix of the elastic boundary are first derived based on the finite element method, and then a coupled vibroacoustic model is developed to calculate the acoustic properties of the structure. A comprehensive study is performed to highlight the effect of the temperature loading position, temperature range, and heated area on the acoustic radiation responses of composite laminated plates with different elastic supports. The results show that the existence of thermal stress has a great influence on the acoustic radiation of the structure at low frequencies, which is affected by the boundary constraints and heated areas.

1. Introduction

To date, laminated composite plates have been widely used in many areas, such as aeronautical, ocean, and civil engineering applications because of their good performance characteristics, such as high specific stiffness to weight and low maintenance cost. These structures are often exposed to the thermal environment during their service life, due to which thermal stresses may be induced; then, these structures may experience buckling and dynamic instability. Therefore, the acoustic radiation behaviour of composite laminated plates in thermal environments is of great technical importance in predicting structural performance.

A few studies on the vibration and sound radiation characteristics of laminated composite shells subjected to thermal environments have been reported in the literature. Panda and Singh [1] carried out a nonlinear free vibration analysis of shells considering postbuckling for a uniform temperature field. Yang et al. [2] analytically investigated the vibroacoustic responses of functionally graded (FG) plates

subjected to a thermal environment. Li et al. [3] employed the mode superposition method to obtain a formulation for the sound transmission loss of a simply supported composite plate and studied in detail the effect of the thermal environment, elevation angle, and azimuth angle of incident sound on the sound transmission loss of composite plates. To improve the acoustic characteristics of a four-edge clamped bimaterial plate, Yang et al. [4] addressed the optimization of radiated acoustic power in different thermal environments in nearby frequency bands, and they studied the sum of the acoustic power at the first two resonance frequencies. Li et al. [5] focused on the application of the method of the piecewise shear deformation theory for the analytical solution of a clamped rectangular sandwich panel in a thermal environment and compiled an exhaustively detailed summary of the dynamic and acoustic radiation characteristics and sound transmission loss of a sandwich plate in thermal environments. Zhou et al. [6] used a simplified closed-form method to investigate the dynamic and acoustic responses of a rectangular plate subjected to thermomechanical loads. The advantage of this approach is

that it can work with some combinations of classical boundary conditions, such as simply supported and clamped boundary conditions and a few cases involving free edges. Huang et al. [7] developed a vibration-acoustic model of simply supported shape memory alloy (SMA) composite laminate plates considering the prestaining of SMA and the thermal expansion force of graphite-epoxy resin. Li and Li [8] derived theoretical formulations for the vibration and sound radiation of a simply supported asymmetric laminated plate considering the effects of thermal environments. Sharma et al. [9] developed a general mathematical model for computing the vibroacoustic behaviour of laminated composite panels under the framework of higher-order shear deformation theory, and the effects of different structural parameters, several classical support conditions, and various material properties on the acoustic radiation response of laminated composite plates under harmonic central and eccentric excitation were fully discussed. Furthermore, these scholars [10] also reported the vibration and acoustic responses of unbaffled laminated composite flat panels excited by harmonic point loading under various support conditions.

From a review of the literature, most previous studies on composite laminated plates have been confined to the classical boundary conditions, such as free, simply supported, clamped, and their combinations. However, a variety of possible boundary supports encountered in practical engineering applications may not always be classical in nature, and there will always be some elasticity along the supports. Moreover, in various realistic scenarios, the temperature distribution on the composite laminated plate is usually uneven. For example, as the hypersonic structure accelerates in the atmosphere, the plate boundary acts as a radiator when connected to the cooler substructure, resulting in aerodynamic heat being generated on its surface [11]. To the best of the authors' knowledge, few scholars have addressed the acoustic performance of composite laminated plates with elastic boundaries subjected to local thermal loads. Over the last several years, the rapid growth in the design of structures and industrial processes has required the development of computational models that reflect practical engineering problems; therefore, it is highly significant to study the acoustic radiation performance of composite laminated plates with arbitrary elastic edge supports subjected to local thermal loads. The motivation of this study is to solve the aforementioned problems.

The paper is arranged in four sections. Following this introduction, Section 2 provides the theoretical background of a composite laminated plate and elastic boundary, and the corresponding matrix representation is given. In Section 3, the effects of the temperature loading position, temperature range, and heated area on the acoustic performance of composite laminated plates subjected to local thermal loading are discussed. The final section summarizes the main results of the paper.

2. Theory

2.1. Governing Equations. As shown in Figure 1, the constitutive equation of a composite laminated plate subjected to thermal loading can be expressed as [12]

$$\{F\} = [D]\{\varepsilon\} - \{F^N\}, \quad (1)$$

where $\{F\}$ is the thermal stress of the laminated plate, $[D]$ is the stiffness matrix of the laminated plate, $\{\varepsilon\}$ is the total strain vector, and $\{F^N\}$ is the thermal internal force vector.

$$\{F\} = \{N_x, N_y, N_{xy}, M_x, M_y, M_{xy}, Q_x, Q_y\}^T, \quad (2)$$

$$\{F^N\} = \{N_x^N, N_y^N, N_{xy}^N, M_x^N, M_y^N, M_{xy}^N, 0, 0\}^T, \quad (3)$$

$$\{\varepsilon\} = \{\varepsilon_x, \varepsilon_y, \gamma_{xy}, \kappa_x, \kappa_y, \kappa_{xy}, \gamma_{xz}, \gamma_{yz}\}^T, \quad (4)$$

$$[D] = \begin{bmatrix} A_{11} & A_{12} & A_{16} & B_{11} & B_{12} & B_{16} & 0 & 0 \\ A_{12} & A_{22} & A_{26} & B_{12} & B_{22} & B_{26} & 0 & 0 \\ A_{16} & A_{26} & A_{66} & B_{16} & B_{26} & B_{66} & 0 & 0 \\ B_{11} & B_{12} & B_{16} & D_{11} & D_{12} & D_{16} & 0 & 0 \\ B_{12} & B_{22} & B_{26} & D_{12} & D_{22} & D_{26} & 0 & 0 \\ B_{16} & B_{26} & B_{66} & D_{16} & D_{26} & D_{66} & 0 & 0 \\ 0 & 0 & 0 & 0 & 0 & 0 & H_{44} & H_{45} \\ 0 & 0 & 0 & 0 & 0 & 0 & H_{45} & H_{55} \end{bmatrix}, \quad (5)$$

where $N_x, N_y,$ and N_{xy} are the resultant forces of internal stress in the laminated plate and $M_x, M_y,$ and M_{xy} are the moments at the middle surface of the laminated plate. For convenient expression, (5) is simplified as

$$[D] = \begin{bmatrix} A_{ij} & B_{ij} & 0 \\ B_{ij} & D_{ij} & 0 \\ 0 & 0 & H_{ij} \end{bmatrix}, \quad (6)$$

where $A_{ij}, B_{ij}, D_{ij},$ and H_{ij} are the tensile stiffness, coupling stiffness, bending stiffness, and thickness shear stiffness of the laminated plate, respectively, which can be expressed as

$$\begin{aligned} (A_{ij}, B_{ij}, D_{ij}) &= \sum_{k=1}^n \int_{Z_{k-1}}^{Z_k} (\bar{Q}_{ij})_k (1, z, z^2) dz, \quad i, j = 1, 2, 6, \\ H_{ij} &= k_0 \sum_{k=1}^n \int_{Z_{k-1}}^{Z_k} (\bar{Q}_{ij})_k dz, \quad i, j = 4, 5, \end{aligned} \quad (7)$$

where k_0 is the shear correction coefficient, with a value of 5/6. $[\bar{Q}_{ij}]_k$ is the reduced stiffness coefficient matrix in the direction of the fibre layer of the laminated plate, which can be expressed as

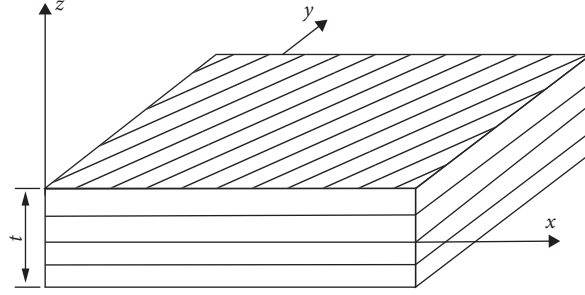


FIGURE 1: Schematic diagram of a composite laminated plate.

$$[Q_{ij}]_k = \begin{bmatrix} Q_{11} & Q_{12} & 0 \\ Q_{12} & Q_{22} & 0 \\ 0 & 0 & Q_{66} \end{bmatrix}, \quad i, j = 1, 2, 6,$$

$$[Q_{ij}]_k = \begin{bmatrix} Q_{44} & 0 \\ 0 & Q_{55} \end{bmatrix}, \quad i, j = 4, 5,$$

$$Q_{11} = \frac{E_{11}}{1 - \nu_{12}\nu_{21}},$$

$$Q_{12} = \frac{\nu_{12}E_{22}}{1 - \nu_{12}\nu_{21}},$$

$$Q_{22} = \frac{E_{22}}{1 - \nu_{12}\nu_{21}},$$

$$Q_{66} = G_{12},$$

$$Q_{44} = G_{13},$$

$$Q_{55} = G_{23}.$$

(8)

The thermal force vector and thermal torque are expressed, respectively, as

$$\{N_x^N, N_y^N, N_{xy}^N\}^T = \sum_{k=1}^n (\bar{Q}_{ij})_k \{e\}_k (z_k - z_{k-1}), \quad (i, j = 1, 2, 6),$$

$$\{M_x^N, M_y^N, M_{xy}^N\}^T = \frac{1}{2} \sum_{k=1}^n (\bar{Q}_{ij})_k \{e\}_k (z_k^2 - z_{k-1}^2), \quad (i, j = 1, 2, 6),$$

(9)

where $\{e\}_k$ is the thermal strain of the k th layer and can be expressed as

$$\{e\}_k = \{e_x, e_y, e_{xy}\}^T = [A] \{\alpha_1, \alpha_2\}_k^T (T_E - T_0), \quad (10)$$

where T_E is the actual temperature, T_0 is the reference temperature, $\{\alpha_1, \alpha_2\}$ is the thermal expansion coefficient, and

$$[A] = \begin{bmatrix} \cos^2 \theta & \sin^2 \theta \\ \sin^2 \theta & \cos^2 \theta \\ \sin 2\theta & -\sin 2\theta \end{bmatrix}. \quad (11)$$

The shape function of the element displacement field is

$$\{U\} = [N] \{d^e\},$$

$$[N] = [N_1 \quad N_2 \quad N_3 \quad N_4]. \quad (12)$$

The total potential energy is the sum of the bending strain energy of the laminated plate and the potential energy of the laminated plate under the action of in-plane forces due to the thermal load, which can be expressed as [13]

$$\Pi = V + P, \quad (13)$$

where V is the bending strain energy of the laminated plate and P is the potential energy of the laminated plate. These equations can be written as

$$V = \frac{1}{2} \iint \left[\{\varepsilon\}^T [A] \{\varepsilon\} + \{\varepsilon\}^T [B] \{\kappa\} + \{\kappa\}^T [B] \{\varepsilon\} + \{\kappa\}^T [D] \{\kappa\} + \{\gamma\}^T [H] \{\gamma\} \right] dA,$$

$$P = \frac{1}{2} \iint \left[N_x \left(\frac{\partial w}{\partial y} \right)^2 + 2N_{xy} \left(\frac{\partial w}{\partial y} \right) \times \left(\frac{\partial w}{\partial y} \right) + N_y \left(\frac{\partial w}{\partial y} \right)^2 \right] dx dy.$$

(14)

The derivative of this function with respect to the degree of freedom vector can be obtained for the composite plate

structure, giving the stiffness matrix and the stress matrix caused by thermal load.

2.2. Radiated Acoustic Power Forecast Model. As shown in Figure 2, the general equation of motion for a composite laminated plate with elastic supports subjected to the local temperature is

$$\{-\omega^2[M] + i\omega[C] + [K]\}U(\omega) = \{F\}, \quad (15)$$

where $[M]$ and $[K] = [K_s] + [K_b] + [K_\sigma]$ are the global mass matrices and global stiffness matrices of a composite laminated plate, respectively, where $[K_s]$ is the stiffness matrix of the stiffened plate and $[K_b]$ is the stiffness matrix of the boundary element of the stiffened plate, including the elastic support boundary k_t and rotation boundary k_r . The derivation of boundary rotational stiffness and boundary support stiffness can be found in our previous work [14]. ω represents the vibration frequency, $\{U\}$ represents the generalized displacement vector of the finite locally resonant plate, and $\{F\}$ is an external harmonic excitation.

We denote $[B] = -\omega^2[M] + i\omega[C] + [K]$, and the nodal velocity vector at each of the nodes in the finite locally resonant plate can be expressed by

$$v = i\omega U(\omega) = i[B]^{-1}\{F\}. \quad (16)$$

By using the transformation matrix method, the following expression of the normal velocity on the finite locally resonant plate can be used as the boundary condition for the Rayleigh integral:

$$v_n(\omega) = i\omega[D][B]^{-1}\{F\}, \quad (17)$$

where $[D]$ is a transformation matrix.

As shown in Figure 3, when the surface normal velocity of a planar rectangular plate is known, the generated radiated acoustic pressure can be calculated using the Rayleigh integral on the assumption that the plate is surrounded by an infinite, coplanar baffle [15]:

$$P(\vec{r}_{s'}) = \frac{i\omega\rho_a}{2\pi} \int_{s_1} v_n(\vec{r}_s) \frac{e^{-ikR}}{R} ds, \quad (18)$$

where $r_{s'}$ and r_s represent the position of the observation point and elemental surface δ_s with the normal velocity $v_n(\vec{r}_s)$, respectively. $R = |r_{s'} - r_s|$, k is the acoustic wave-number, and ρ_a is the density of the fluid.

In the far field, the time averaged acoustic intensity of the structure is given by the following expression:

$$I = \frac{|P(\vec{r}')|^2}{2\rho c}. \quad (19)$$

Hence, if the radius of the hemisphere is twenty times the largest dimension of the vibrating structure, the sound power W radiated into the semi-infinite space above the plate is the integral of the sound intensity and can be written as

$$W = \int_0^{2\pi} \int_0^{\pi/2} I \cdot R^2 \sin \theta d\theta d\phi. \quad (20)$$

With the numerical discrete method, the radiated acoustic power can be evaluated over each of the total surface elements [16]:

$$w = \sum_{i=1}^{N_\theta} \sum_{j=1}^{N_\phi} \frac{|P(R, \tilde{\theta}_i, \tilde{\phi}_j)|^2}{2\rho c} R^2 \sin(\tilde{\theta}_i) \delta\theta \delta\phi, \quad (21)$$

where $\delta\theta = (\pi/2N_\theta)$; $\delta\phi = (2\pi/N_\phi)$; $\tilde{\theta}_i = i\delta\theta$; $\tilde{\phi}_j = j\delta\phi$.

The mean square velocity of the stiffened plate can be calculated from the following formulas:

$$\begin{aligned} \bar{v}_n^2 &= \frac{1}{s} \int_s v_n^2 ds, \\ \sigma &= \frac{W}{(1/2)\rho_a c_a a b \langle \bar{v}_n^2 \rangle}, \end{aligned} \quad (22)$$

where ρ_a is the fluid density, c_a is the sound velocity, a is the plate length, and b is the plate width.

3. Numerical Results and Discussion

A schematic diagram of the composite laminated plate subjected to local thermal loading and the coordinate system is shown in Figure 2. The composite laminated plate is made of carbon/epoxy with the following material and geometric properties (unless otherwise stated). The physical material parameters and structural dimensions of the laminated plate are as follows: density $\rho = 1520$ (kg/m³), $E_1 = 133.86$ GPa, $E_2 = 7.706$ GPa, $G_{12} = 4.302$ GPa, $\nu_{12} = 0.301$, $\alpha_1 = 0.32E - 6^\circ\text{C}^{-1}$, $\alpha_2 = 25.89E - 6^\circ\text{C}^{-1}$, and $\alpha_3 = 0K^{-1}$. The layer of the alternately composite laminated plate is [0/90/0/90/90/0/90/0]; the length, width, and thickness of the laminated plate are represented by a , b , and t , respectively; the size of the heated area is in the form of a_0 and b_0 ; and the distances between the centre of the heated area and the border of the laminated plates are denoted by d_1 and d_2 . The boundary support stiffness and boundary rotational stiffness are unchanged along the boundary of the composite laminated plate, all boundary support stiffnesses are denoted by k_t , and the boundary rotational stiffness can be denoted by K_r . The modal damping ratio of the structure is 0.01.

3.1. Model Validation. To verify the accuracy of the model, the sound pressure levels of a laminated plate are calculated and compared with those in the literature [11]. The geometric dimensions and physical parameters are as follows: $a = 0.15$ m, $b = 0.15$ m, $\rho = 1420.05$ kg/m³, and $t = 0.002$ m. The layer of the alternately composite laminated plate is [0/90/0/90/0/90], $E_1 = 7.205$ GPa, $E_2 = 6.327$ GPa, $G_{12} = 2.8$ GPa, $G_{13} = 2.8$ GPa, $G_{23} = 1.4$ GPa, $\nu_{12} = 0.17$, and $\alpha_3 = 0K^{-1}$. The initial temperature is $T_0 = 293.15K^{-1}$, the grid is 48×48 , and the sound pressure levels of a laminated plate under CFFF boundary conditions are shown in Figure 4 (F represents a free boundary, and c represents a rigid fixed boundary). The support stiffness and rotation stiffness are assumed to be infinite to represent the rigid fixed boundary. Similarly, the support stiffness and rotation stiffness are taken to be small values to represent the free boundary. From Figure 4, the computed result is in good agreement with the results in the literature [10], except in the frequency range of 250 Hz to 350 Hz, and the deviation is

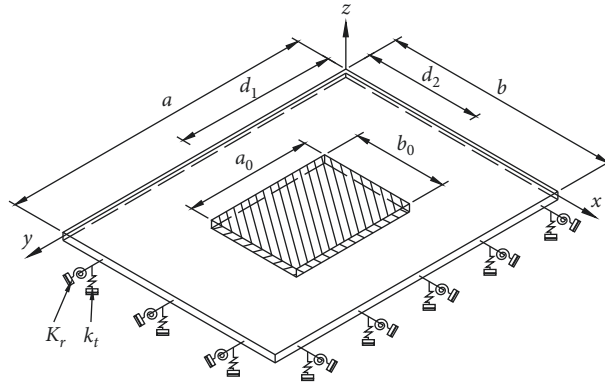


FIGURE 2: Locally heated laminated plate with elastic boundary subjected to local thermal load.

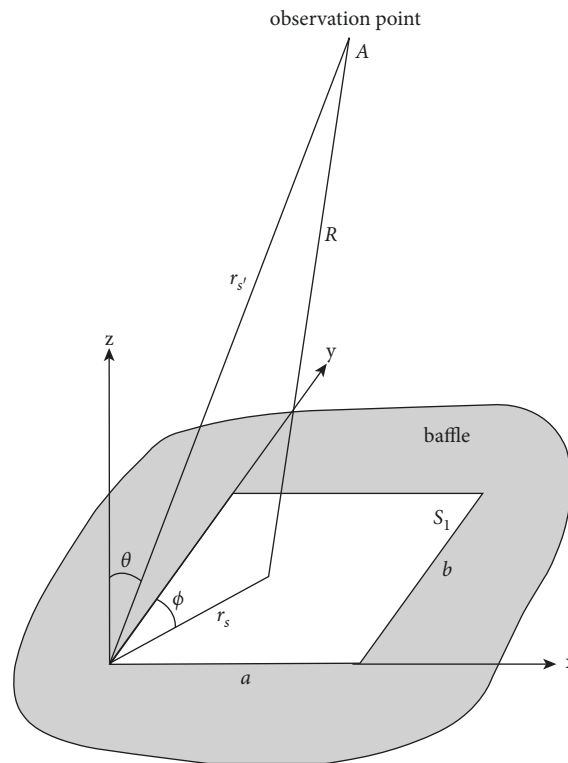


FIGURE 3: Rayleigh integral coordinate.

caused by the limitation of displacement boundary conditions applied to the structure in the experiment.

3.2. Acoustic Performance of a Composite Laminated Plate under Local Thermal Loading

3.2.1. Influence of the Temperature Loading Position. The size of the laminated plate is set as $a = 0.5 \text{ m}$, $b = 0.5 \text{ m}$, $t = a/80$, $k_r = 0 \text{ (N/rad)}$, $a_0 = 0.4a$, and $b_0 = 0.4b$, and the unit harmonic excitation point is selected at location $(x, y) = (0.21 \text{ m}, 0.25 \text{ m})$ (the same below) with reference to Figure 2. The heated area is sixteen percent of the total area of the laminated plate, the position of the temperature load

varies from $d_1 = 0.2a$ to $d_1 = 0.4a$, and the temperature load is the critical temperature of the laminate structure when $d_1 = 0.5a$. The mean square velocity, sound radiation efficiency, and sound power level curves are shown in Figure 5–7, respectively. The first peak of the mean square velocity curve moves little to low frequency when the boundary constraint is small ($k_t = 4e5 \text{ N/m}^2$), the second peak decreases and moves in the high frequency direction owing to the uneven distribution of thermal stress generated by the local temperature in the laminated plate, and the thermal stress stiffness is smaller than that of the laminated plate. When the boundary constraint is enhanced ($k_t = 1e15 \text{ N/m}^2$), the first and third peak values of the mean

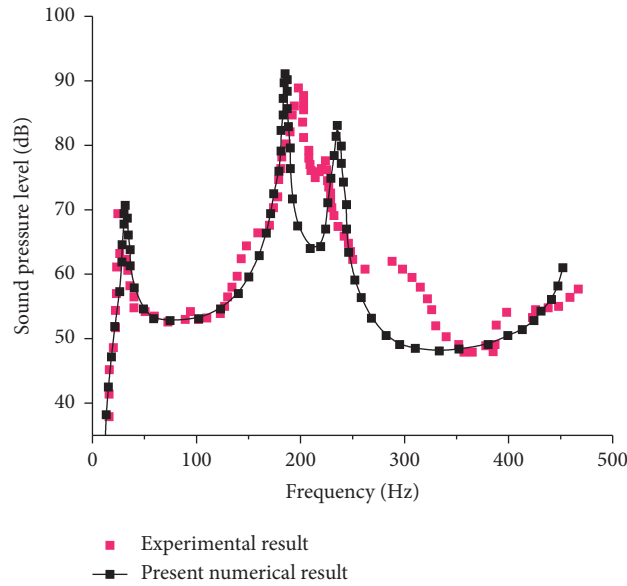


FIGURE 4: Experimental validation study of sound pressure levels for the laminated plate.

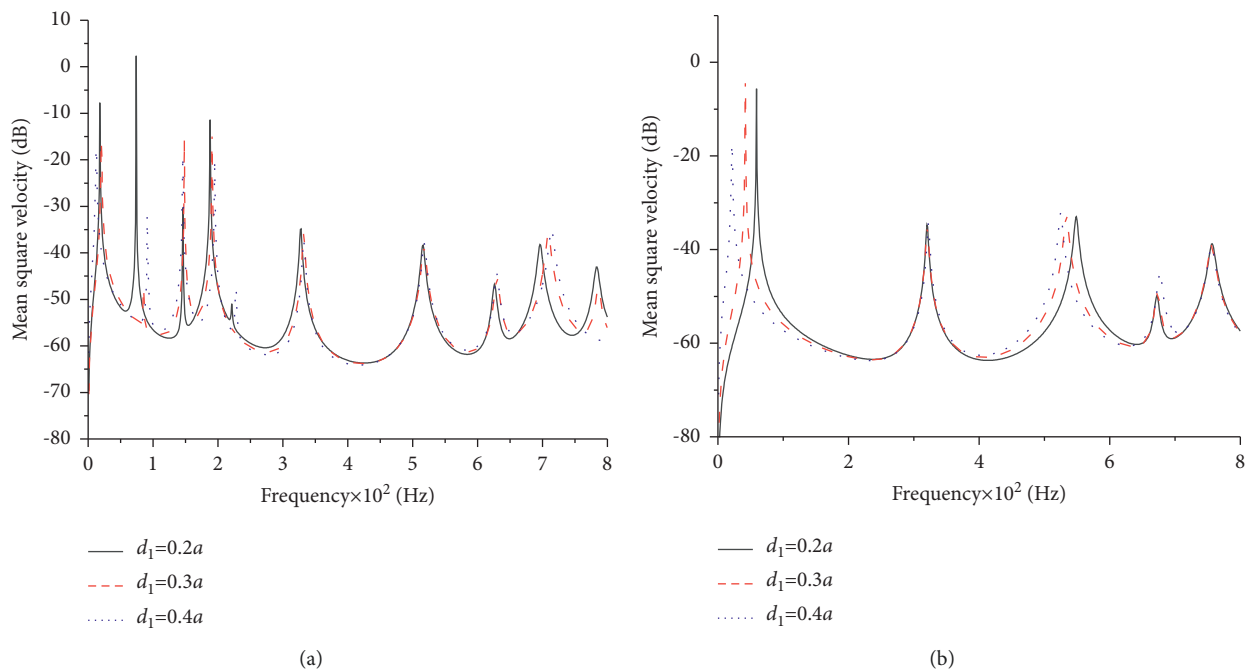


FIGURE 5: Mean square velocity of laminated plates with different heating positions. (a) $k_t = 4e5N/m^2$. (b) $k_t = 1e15N/m^2$.

square velocity curve move to low frequency, and the mean square velocity decreases at the first-order frequency, while there is no significant change at other order frequencies. This is because the thermal stress of laminated plates generated by the local temperature load is negative when the boundary constraints are large. The acoustic radiation efficiency of the laminated plate changes little when the temperature loading

position is different, regardless of the small boundary restraint or larger boundary constraints. The temperature loading position has a great influence on the radiated sound power level in the low frequency range. For example, the radiation sound power at the first-order frequency decreases significantly in laminated plates and moves to a low frequency when $k_t = 1e15N/m^2$ because the thermal stress is

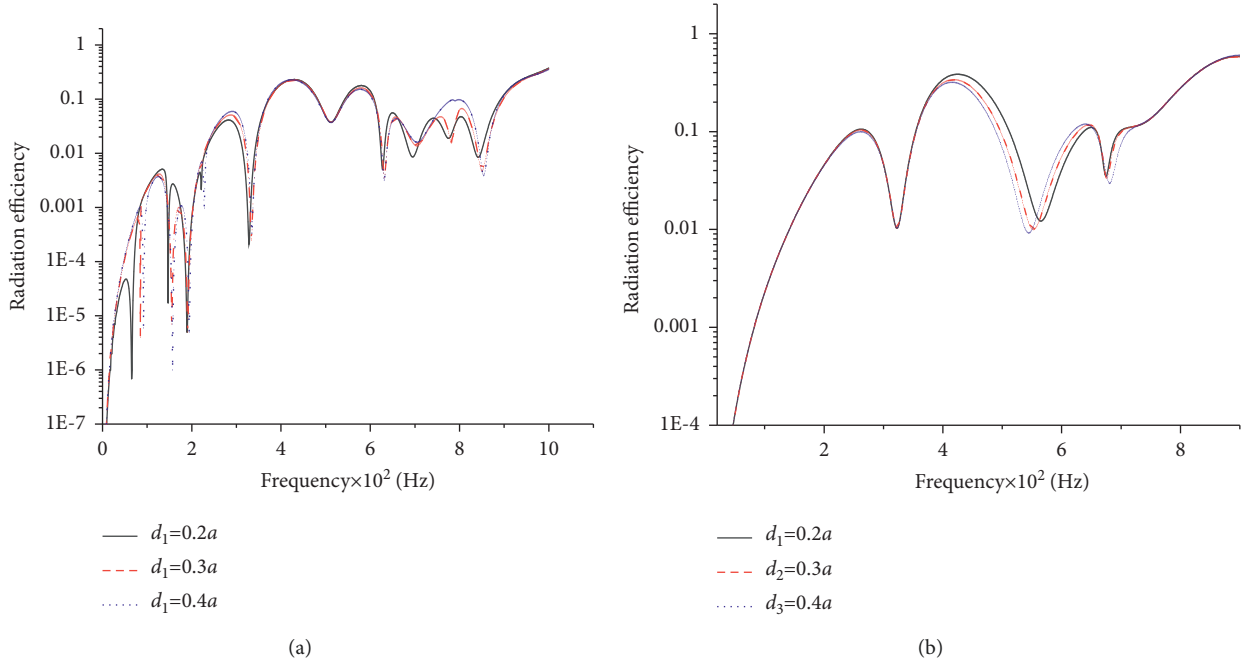


FIGURE 6: Sound radiation efficiency of laminated plates with different heating positions. (a) $k_t = 4e5N/m^2$. (b) $k_t = 1e15N/m^2$.

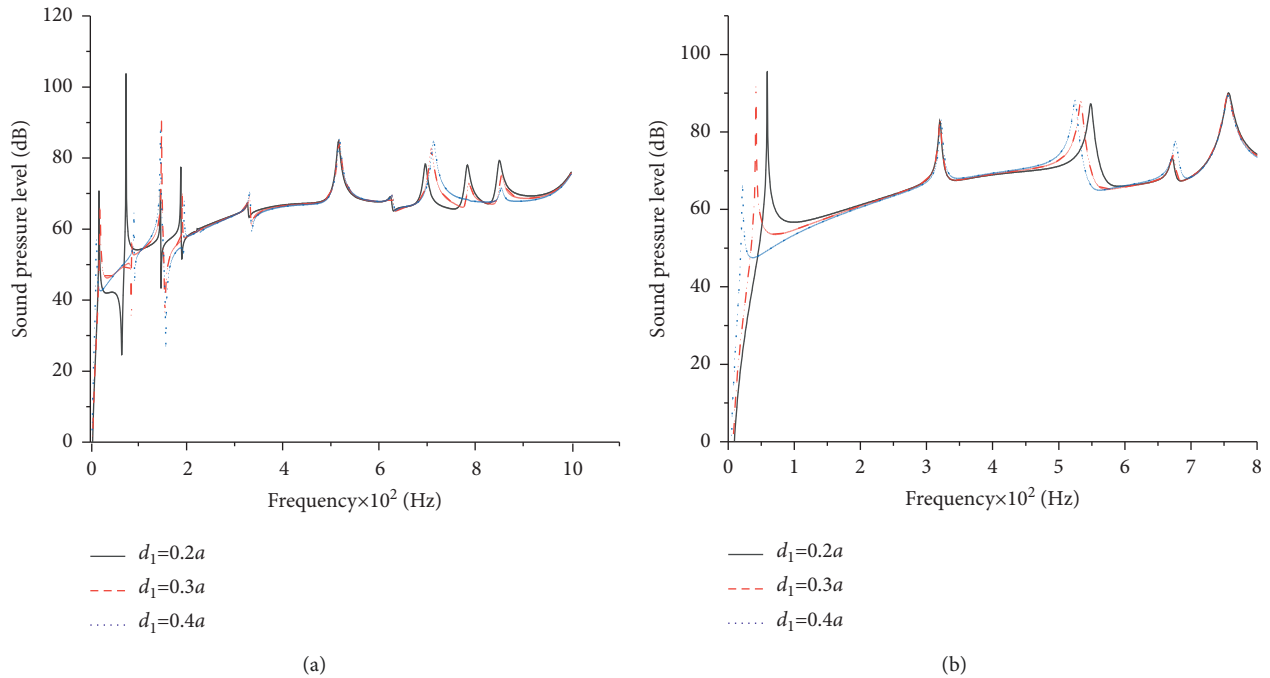


FIGURE 7: Sound power level of laminated plates with different heating positions. (a) $k_t = 4e5N/m^2$. (b) $k_t = 1e15N/m^2$.

higher if the temperature loading location is close to the centre position of laminated plates when the boundary constraints are large.

3.2.2. *The Influence of Temperature.* The heating range is the entire laminate area, T_{cr} is the critical temperature, and the

boundary conditions are $k_t = 1e8N/m^2$ and $k_r = 1e6N/rad$. The mean square velocity, sound radiation efficiency, and sound power level curves are shown in Figure 8–10, respectively. From the figures, the mean square velocity curve of the laminated plate moves to low frequency, and the peak value of the mean square velocity increases. Additionally, the sound radiation efficiency of the laminated plates decreases

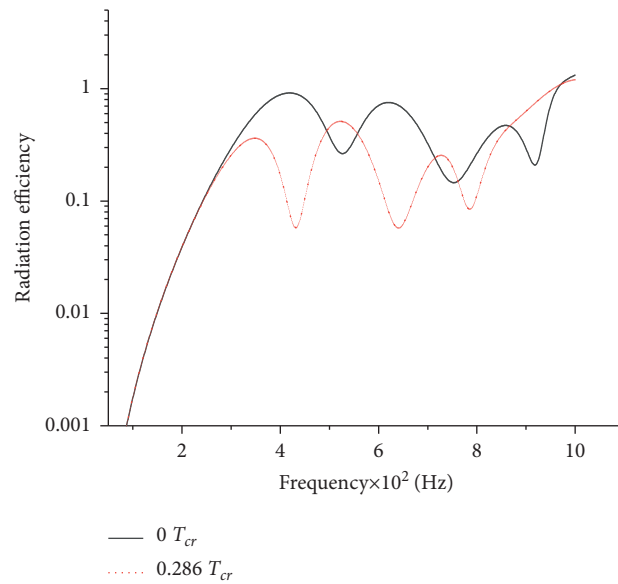


FIGURE 8: Sound radiation efficiency of laminated plates in different thermal environments.

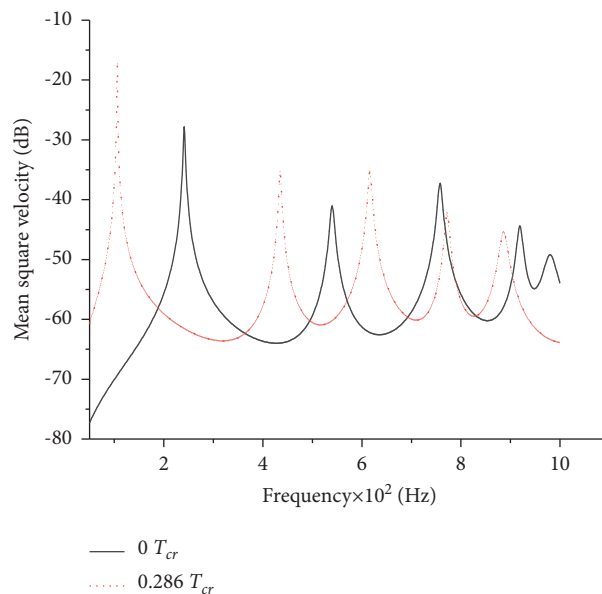


FIGURE 9: Mean square velocity of laminated plates in different thermal environments.

and moves to the low frequency. This happens because the temperature “softens” the integral stiffness of the laminated plates, and the radiated acoustic power level curve of the laminated plates moves to a low frequency. However, the peak of the radiated acoustic power level curve demonstrates no obvious change.

3.2.3. *Heated Area.* The average temperature of the laminate is kept constant, and the boundary conditions are $k_t = 1e8N/m^2$ and $k_r = 1e6N/rad$. The heated area is $A = a \times b$ and $A = 0.4a \times 0.4b$. The temperature loads are $T = 0.11T_{cr}$ and $T = 0.69T_{cr}$. The mean square velocity, sound radiation efficiency, and sound power level curves

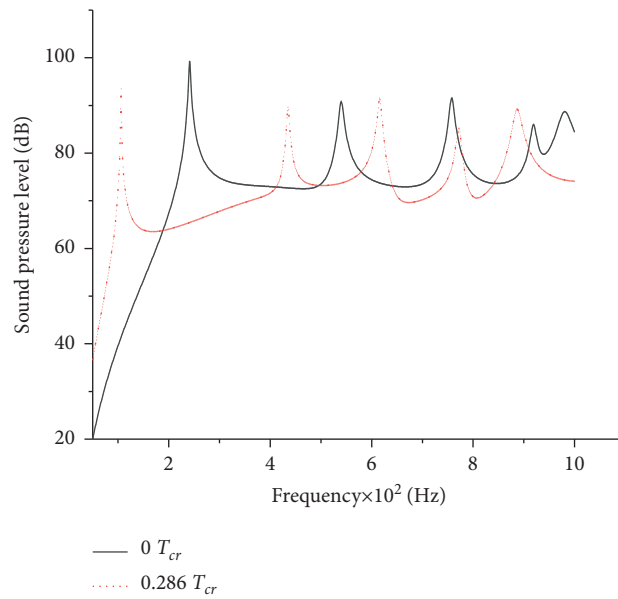


FIGURE 10: Sound power level of laminated plates in different thermal environments.

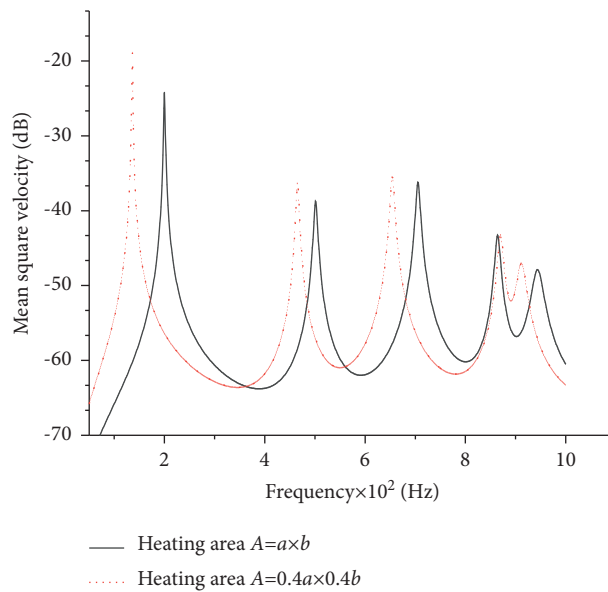


FIGURE 11: Mean square velocity of laminated plates with different heating areas.

are shown in Figure 11–13, respectively. From the figures, the mean square velocity curve moves to low frequency, and the sound radiation efficiency decreases and moves to low frequency when the heated area decreases. The radiation sound power curve integral moves to low

frequency. In other words, the smaller the heated area, the greater the influence of the temperature load on the acoustic radiation performance of the laminated plate when the laminated plate is averaged at constant temperature.

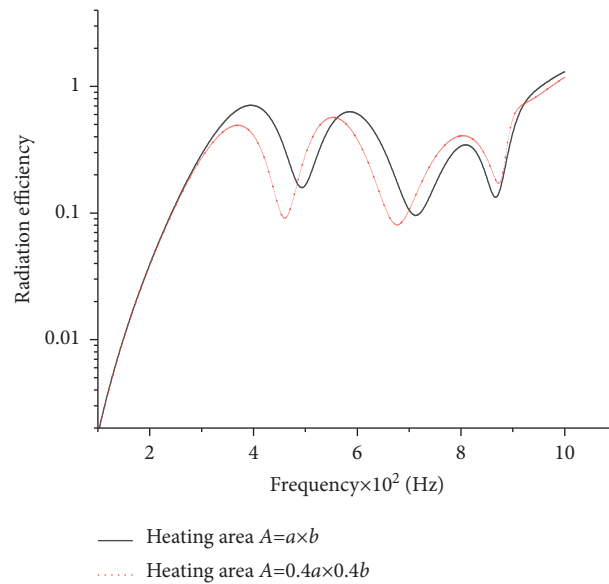


FIGURE 12: Sound radiation efficiency of laminated plates with different heating areas.

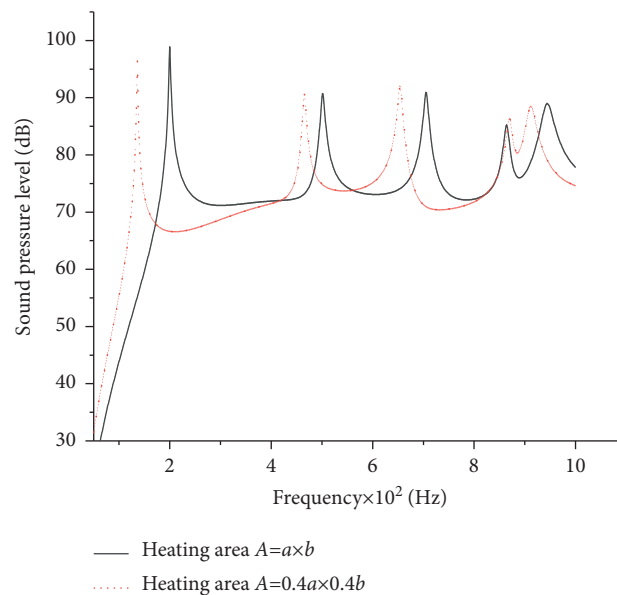


FIGURE 13: Sound power level of laminated plates with different heating areas.

4. Summary

In this paper, the calculation model of vibration and acoustic radiation of a laminated structure under arbitrary boundary conditions under local thermal loading is established, and the influence of boundary conditions, heating location, and heating area on the acoustic radiation performance of the laminated structure is studied. The main conclusions are as follows:

- (1) The presence of thermal stress has a great influence on structural acoustic radiation, especially at low frequencies.

- (2) The stronger the boundary constraint, the more significant the influence of thermal stress on structural acoustic radiation.
- (3) The smaller the heated area, the greater the influence of the temperature load on the acoustic radiation performance of the laminated plate when the laminated plate is averaged at constant temperature.

Data Availability

All data generated or analysed during this study are included within the article.

Conflicts of Interest

The authors declare that there are no conflicts of interest regarding the publication of this paper.

Acknowledgments

This project was supported by the Science and Technology Research Program of Chongqing Municipal Education Commission (grant no. KJQN202100746).

References

- [1] S. K. Panda and B. N. Singh, "Large amplitude free vibration analysis of thermally post-buckled composite doubly curved panel using nonlinear FEM," *Finite Elements in Analysis and Design*, vol. 47, no. 4, pp. 378–386, 2011.
- [2] T. Yang, W. Zheng, Q. Huang, and S. Li, "Sound radiation of functionally graded materials plates in thermal environment," *Composite Structures*, vol. 144, pp. 165–176, 2016.
- [3] X. Li, K. Yu, R. Zhao, J. Han, and H. Song, "Sound transmission loss of composite and sandwich panels in thermal environment," *Composites Part B: Engineering*, vol. 133, pp. 1–14, 2018.
- [4] X. Yang and Y. Li, "Structural topology optimization on sound radiation at resonance frequencies in thermal environments," *Science China Physics, Mechanics & Astronomy*, vol. 58, no. 3, pp. 1–12, 2015.
- [5] X. Li, K. Yu, and R. Zhao, "Vibro-acoustic response of a clamped rectangular sandwich panel in thermal environment," *Applied Acoustics*, vol. 132, pp. 82–96, 2018.
- [6] K. Zhou, J. Su, and H. Hua, "Vibration and sound radiation analysis of rectangular plates resting on Winkler foundation in thermal environment with closed form solutions," *Noise Control Engineering Journal*, vol. 65, no. 5, pp. 488–498, 2017.
- [7] Y. Huang, Z. Zhang, C. Li, J. Wang, Z. Li, and K. Mao, "Sound radiation of orthogonal antisymmetric composite laminates embedded with pre-strained SMA wires in thermal environment," *Materials*, vol. 13, no. 17, p. 3657, 2020.
- [8] W. Li and Y. Li, "Vibration and sound radiation of an asymmetric laminated plate in thermal environments," *Acta Mechanica Sinica*, vol. 28, no. 1, pp. 11–22, 2015.
- [9] N. Sharma, T. R. Mahapatra, and S. K. Panda, "Vibro-acoustic behaviour of shear deformable laminated composite flat panel using BEM and the higher order shear deformation theory," *Composite Structures*, vol. 180, pp. 116–129, 2017.
- [10] N. Sharma, T. R. Mahapatra, and S. K. Panda, "Numerical study of vibro-acoustic Responses of un-baffled multi-layered composite structure under various end conditions and experimental validation," *Latin American Journal of Solids and Structures*, vol. 14, no. 8, pp. 1547–1568, 2017.
- [11] W. L. Ko, "Thermal buckling analysis of rectangular panels subjected to humped temperature profile heating," NASA, Washington, DC, USA, NASA/TP, 2004-212041, 2004.
- [12] C. Ray and M. Dey, "Failure analysis of laminated composite plates under linearly varying temperature," *Journal of Reinforced Plastics and Composites*, vol. 28, no. 1, pp. 99–107, 2009.
- [13] A. Avci, Ö. S. Sahin, and M. Uyaner, "Thermal buckling of hybrid laminated composite plates with a hole," *Composite Structures*, vol. 68, no. 2, pp. 247–254, 2005.
- [14] Y. G. Sun, S. Li, and Z. M. Bao, "Sound radiation performance of stiffened plates on elastic foundation with elastic boundary conditions," *Noise and Vibration Control*, vol. 39, no. 1, pp. 16–23, 2019.
- [15] C. E. Wallace, "Radiation resistance of a rectangular panel," *Journal of the Acoustical Society of America*, vol. 51, no. 3B, pp. 946–952, 1972.
- [16] P. Joshi, S. B. Mulani, and R. K. Kapania, "Multi-objective vibro-acoustic optimization of stiffened panels," *Structural and Multidisciplinary Optimization*, vol. 51, no. 4, pp. 835–848, 2015.